Electronic Supplementary Material (ESI) for Journal of Materials Chemistry A.

High performance multicomponent bifunctional catalyst for overall water splitting

Ranjith Bose,[a,b,] Vasanth Rajendran Jothi,[c] K. Karuppasamy,[d] Akram Alfantazi [a,b,*] and Sung Chul Yi [c,e,*]*

[a]Department of Chemical Engineering, Khalifa University, Abu Dhabi, United Arab Emirates.

[b]Nuclear Technology Center, Khalifa University, Abu Dhabi, United Arab Emirates.

[c] Department of Chemical Engineering, Hanyang University, 222 Wangsimni-ro, Seong dong-gu, Seoul 04763, Republic of Korea.

[d]Division of Electronics and Electrical Engineering, Dongguk University-Seoul, Seoul 04620, Republic of Korea.

[e] Department of Hydrogen and Fuel cell technology, Hanyang University, 222 Wangsimni-ro, Seongdong-gu, Seoul 04763, Republic of Korea.

Corresponding author : Dr. Ranjith Bose, Prof. Akram Alfantazi, and Prof. Sung Chul Yi

E-mail id : ranjith.bose@ku.ac.ae, akram.alfantazi@ku.ac.ae & scyi@hanyang.ac.kr

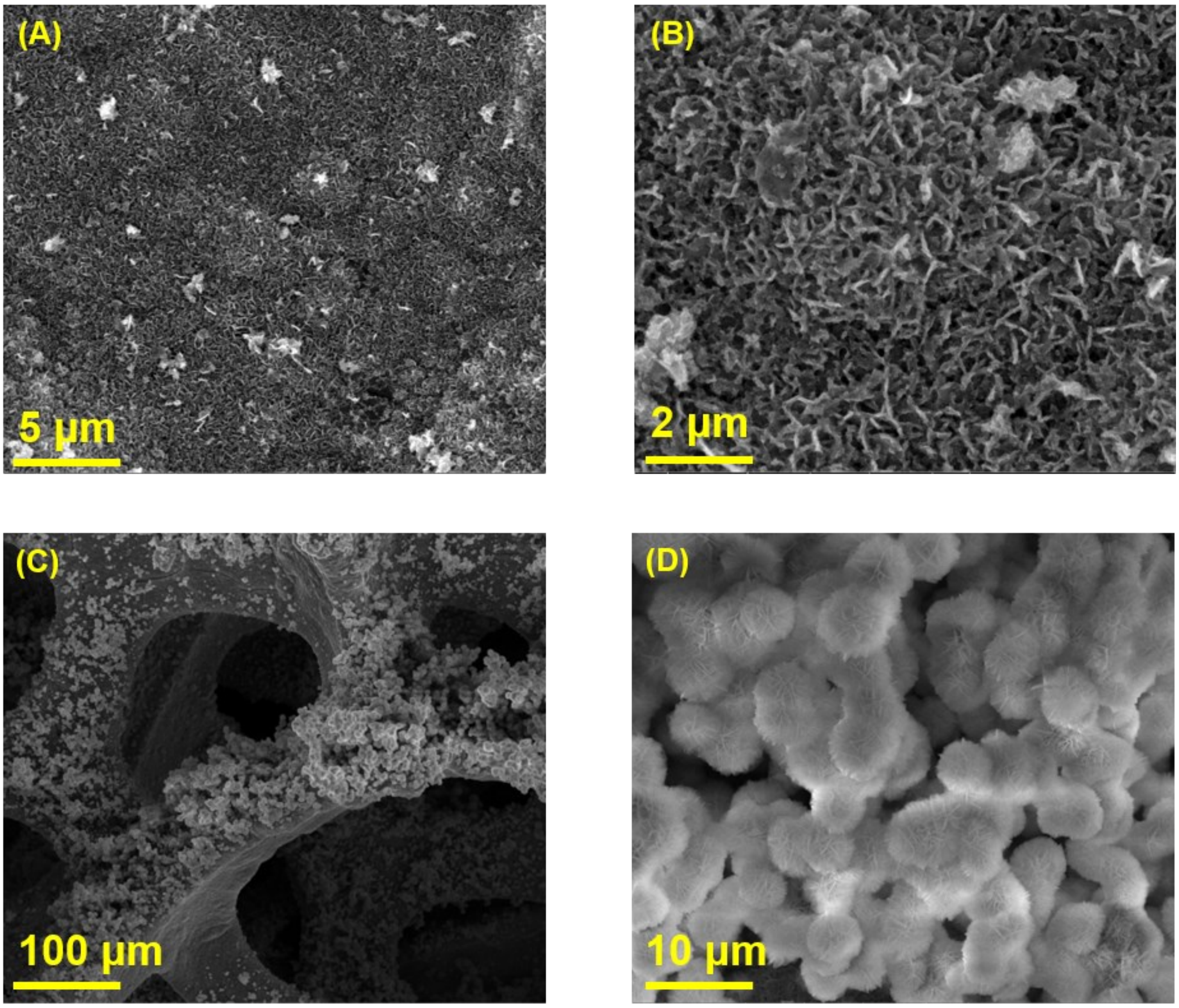

Figure S1. SEM images of (A,B) CoS_x/NF, and (C,D) NiFeOH/NF

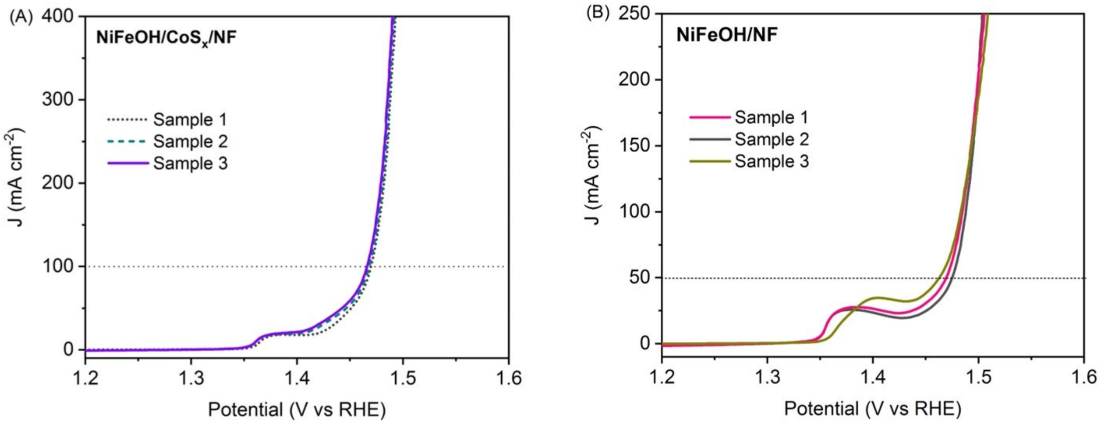

Figure S2. Polarization curve of 3 freshly prepared samples of NiFeOH/CoS_x and NiFeOH, evaluated for reliability.

Samples	NiFeOH/CoS_x	NiFeOH
1	1.45032	1.47047
2	1.44539	1.47577
3	1.44083	1.46301
Average	1.44551	1.46975
Standard deviation	0.00475	0.00641

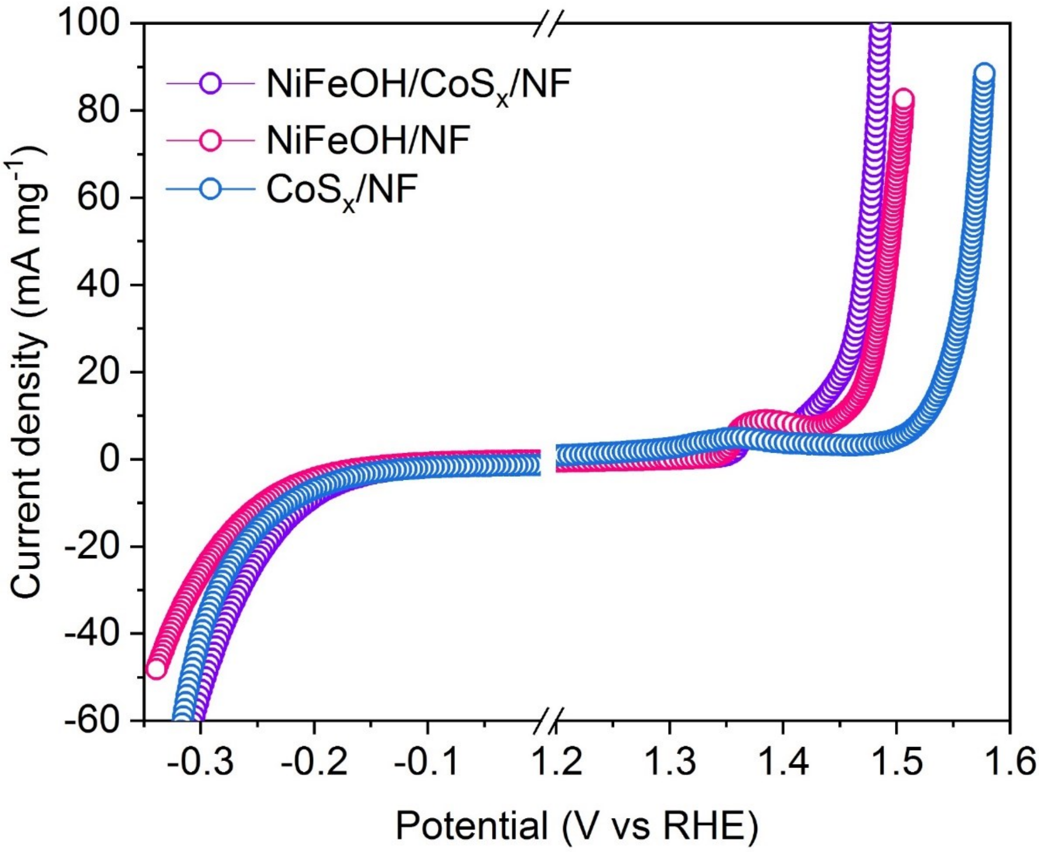

Figure S3. Mass normalized with current density of as-prepared catalysts.

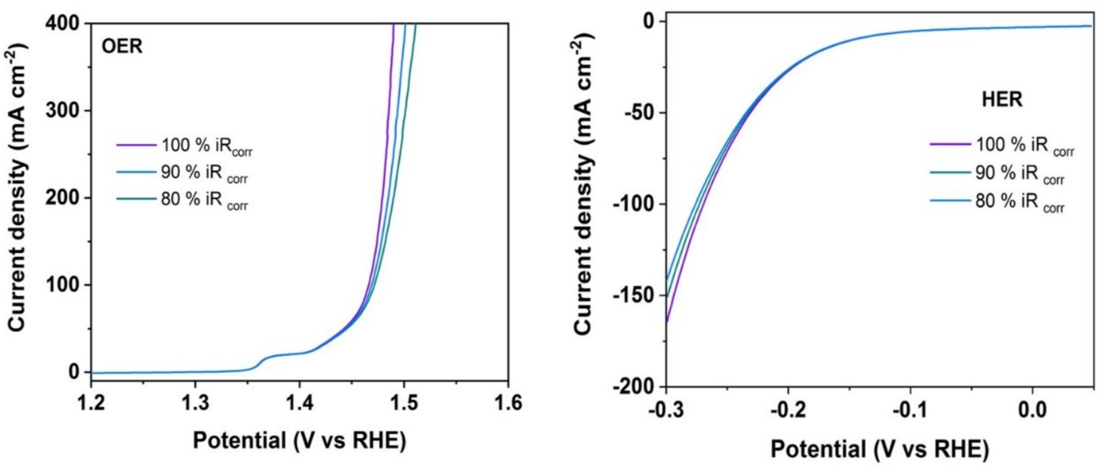

Figure S4. Polarization curves of a NiFeOH/CoS_x/NF electrode in 1 M KOH solution with various percentages of iR drop compensation.

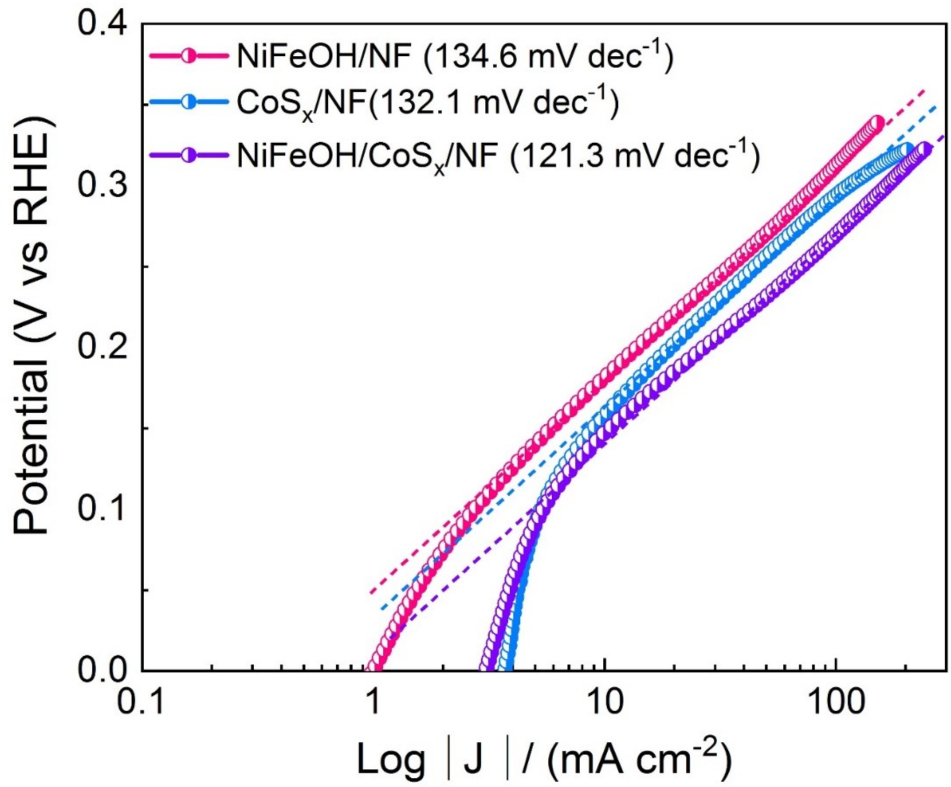

Figure S5. Tafel plots of NiFeOH/CoS_x/NF, CoS_x/NF, and NiFeOH/NF derived from the HER polarization curves.

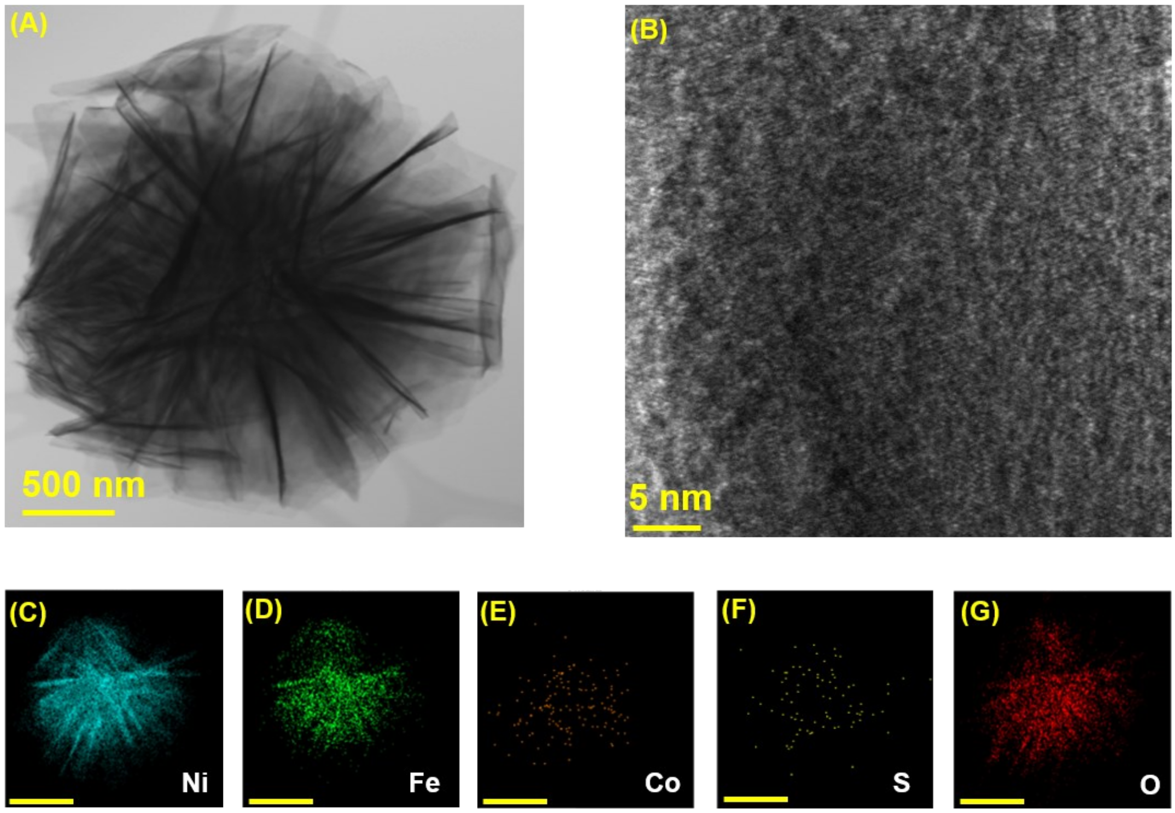

Figure S6. (A,B) HR-TEM images of post HER sample of NiFeOH/CoS_x/NF, (C-G) EDX mapping of Ni, Fe, Co, S and O elements for NiFeOH/CoS_x/NF. Scale bar – 250 nm

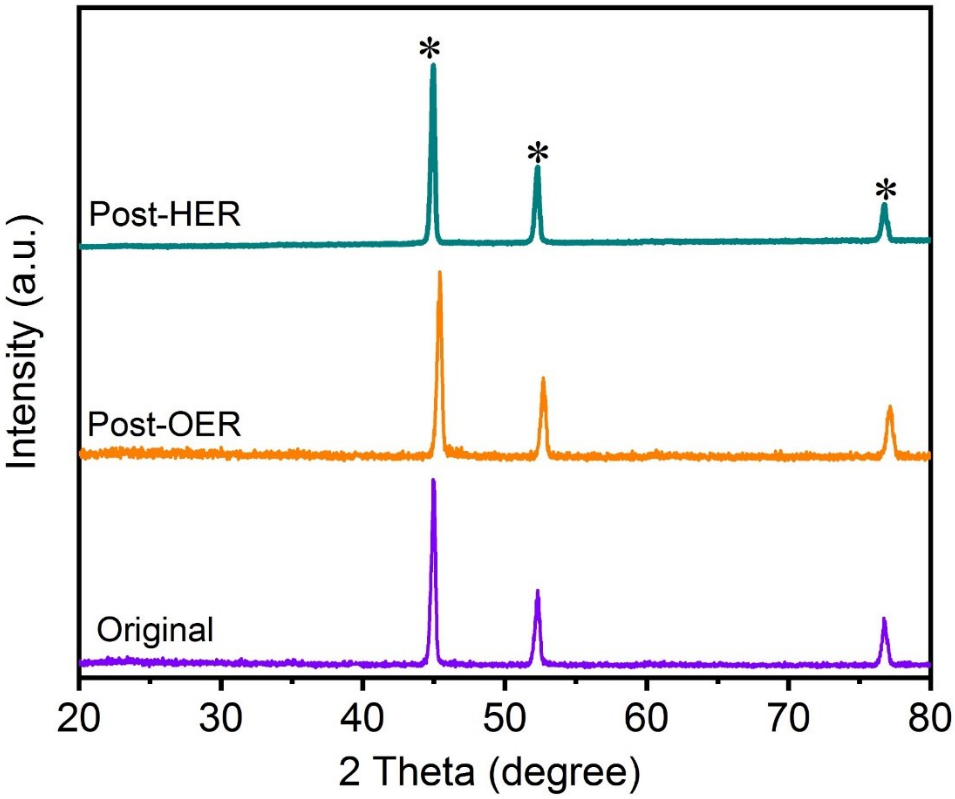

Figure S7. XRD pattern of NiFeOH/CoS_x/NF samples before and after electrocatalytic activity. (Asterisk symbol represented at the peaks of the nickel foam)

The X-ray diffraction (XRD) pattern of CoS_x/NF, and NiFeOH/NF were showed in **Figure S8**. For the CoS_x films, only observed in NF substrate peak, without detection of any CoS_x diffraction peaks. Such an absence of XRD peaks away from those due to the substrate indicates the lack of significant long-range crystalline order, consistent with the previous studies which report on the growth of amorphous CoS_x on FTO substrate via electrodeposition.[1] The XRD pattern of NiFeOH/NF showed a strong diffraction peaks of NF and a three minor peaks at 2θ = 23.72, 35.46, and 39.84 from (020), (101), and (121) planes of $Fe(OH)_3$ (ICPDD card No: 00-046-1436) and FeO(OH) (ICPDD card No: 01-081-0463) respectively.

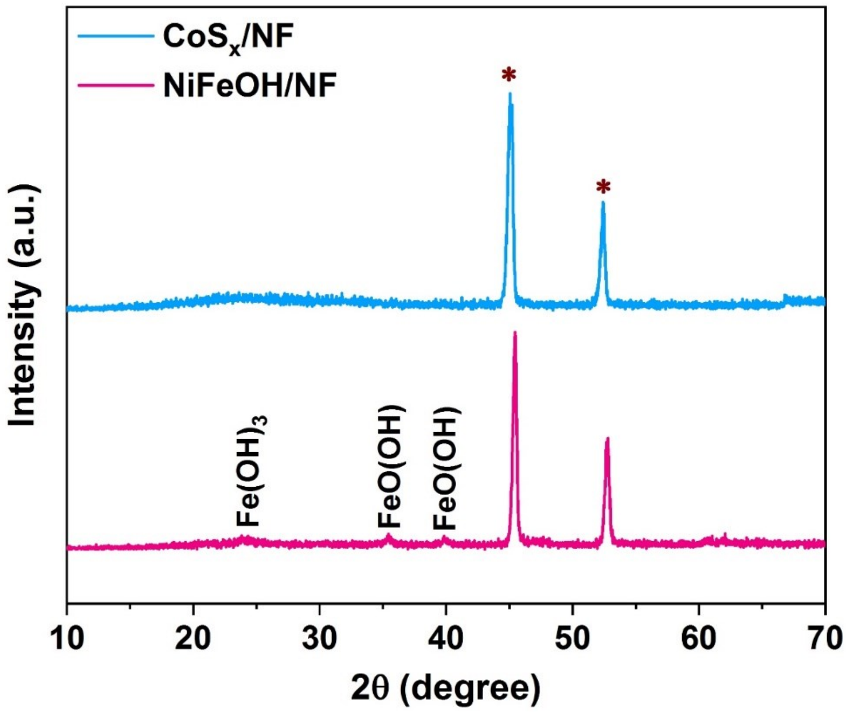

Figure S8. XRD pattern of CoS_x/NF, and NiFeOH/NF samples. (Asterisk symbol represented at the peaks of the nickel foam)

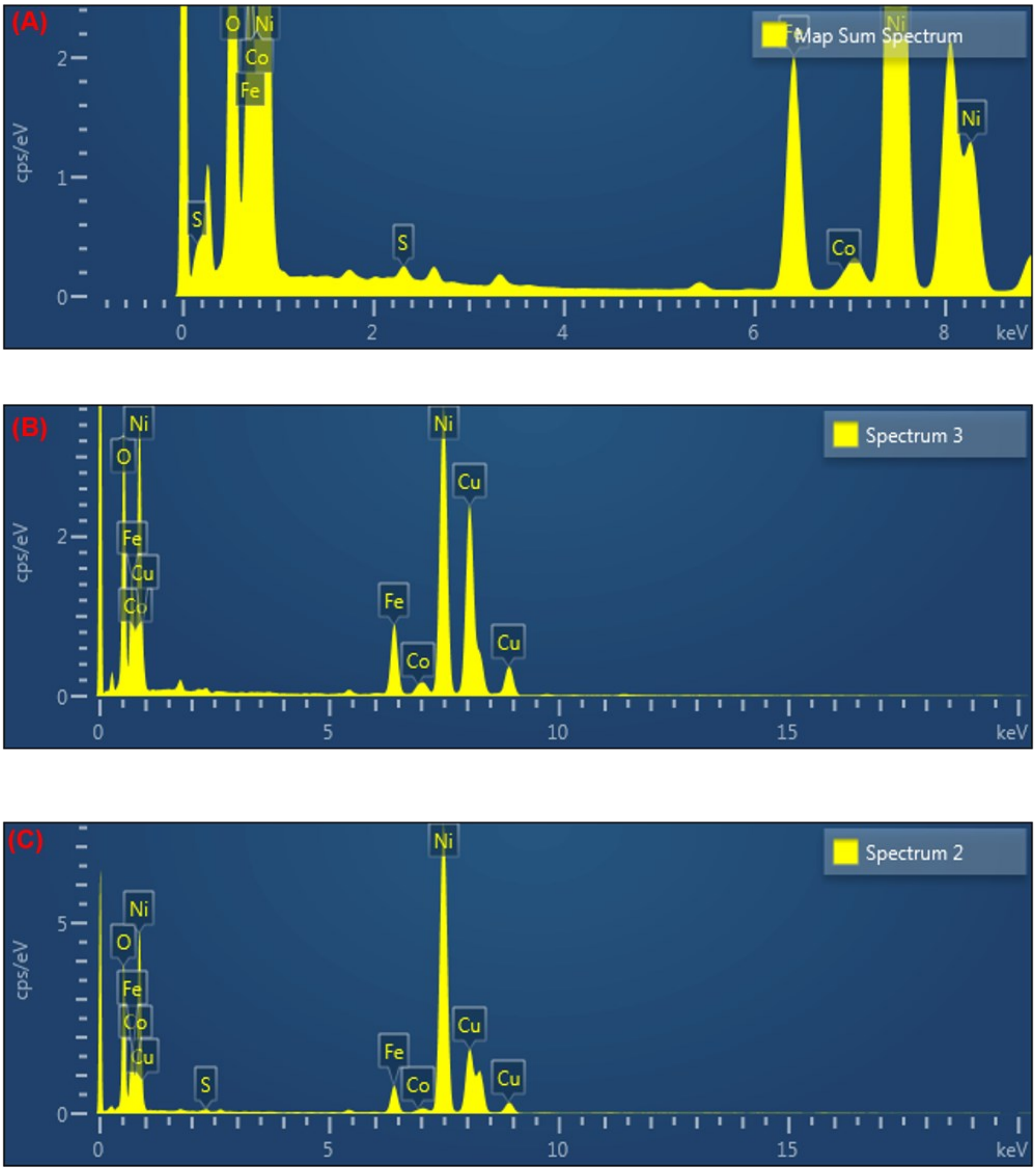

Figure S9. Typical energy-dispersive X-ray spectroscopy (EDX) spectra on the as-made (A), post-OER (B), and post-HER (C) NiFeOH/CoS_x electrocatalysts.

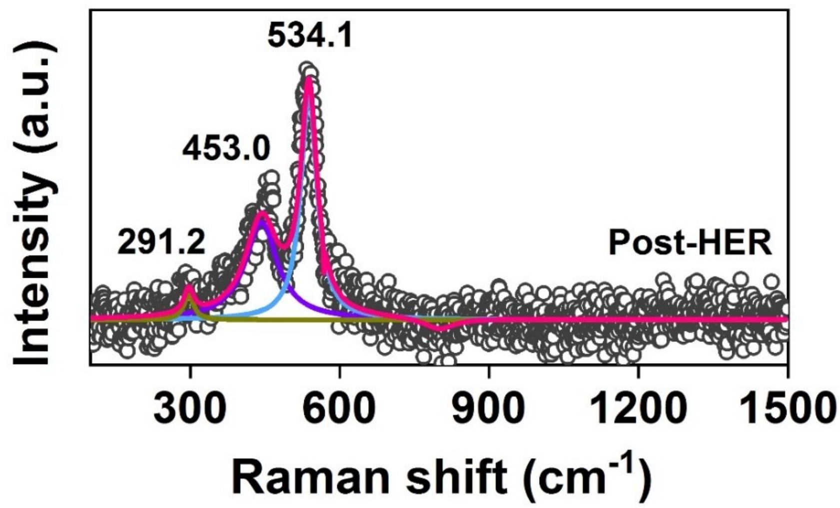

Figure S10. Raman spectra of post-HER NiFeOH/CoS_x/NF electrode

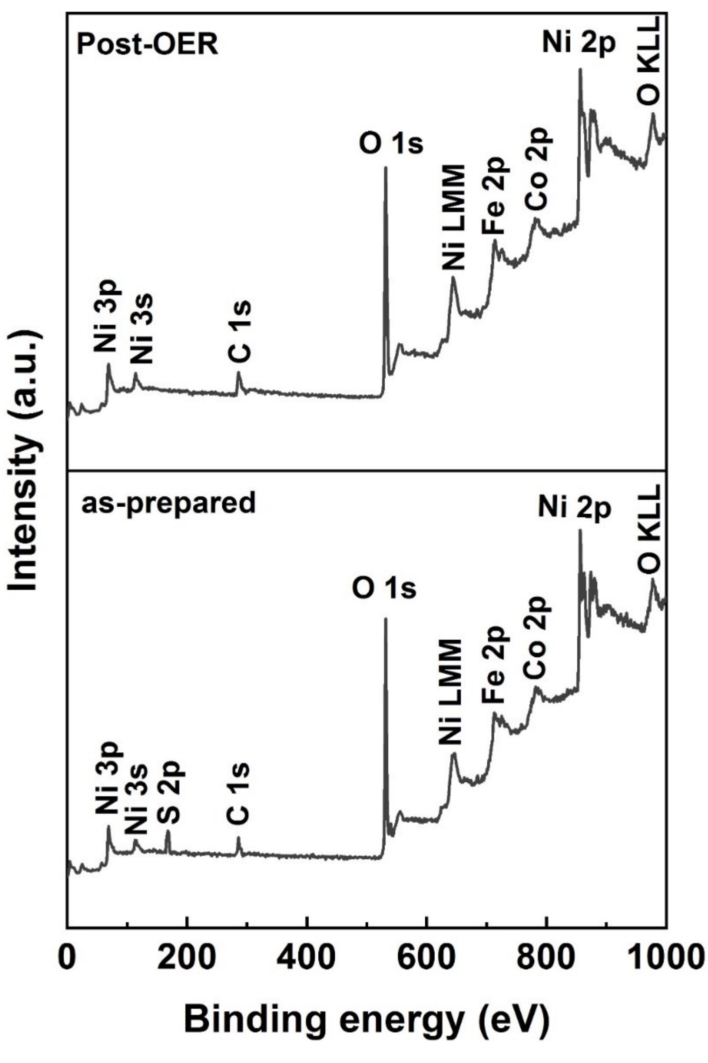

Figure S11. XPS survey spectra of NiFeOH/CoS_x/NF electrode.

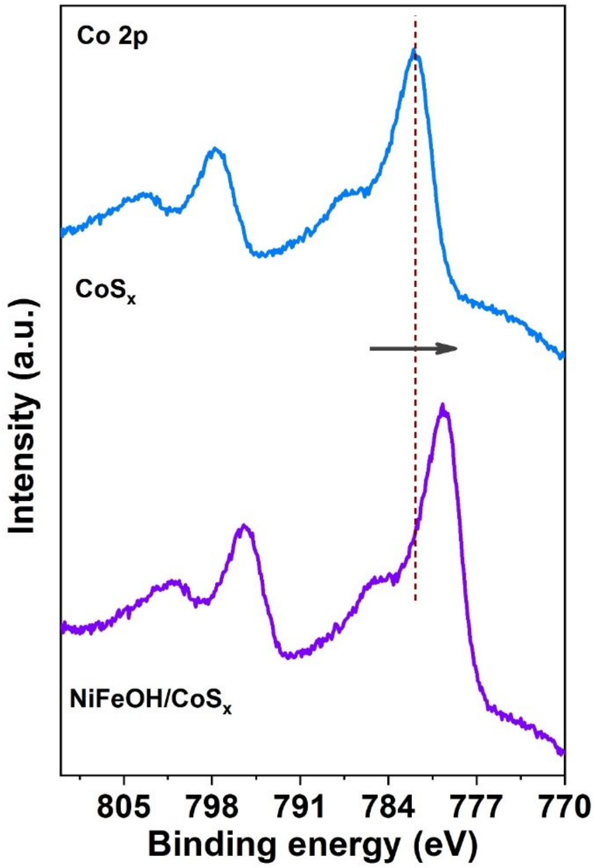

Figure S12. Co 2p spectra of as-prepared NiFeOH/CoS_x and pristine CoS_x

XPS spectra of NiFeOH, and CoS_x were examined and shown in **Figure S13 & S14**. As shown in **Figure S13b** for Ni 2p of NiFeOH, which was deconvoluted into two spin-orbit doublets and two shakeup satellites (identified as "Sat."). The peaks located for first doublet at 854.0 and 871.8 eV and the peaks located for second doublet at 855.7 eV and 873.6 eV were ascribed to the Ni^{2+} / Ni^{3+} for $Ni(OH)_2$/NiOOH, and the corresponding satellite peak, respectively.[2] **Figure S13c** shows the Fe 2p spectra of NiFeOH. The peaks located at 713.3 eV and 725.4 eV for Fe $2p_{3/2}$ and Fe $2p_{1/2}$, respectively, which were assigned as the characteristic peaks of Fe^{3+} in FeOOH.[2] For the O 1s spectra (**Figure S13d**), the peak at 529.4 eV, 530.5 eV, and 532.5 eV can be attributed to oxide, hydroxide, and adsorbed (physical or chemical) water in Ni & Fe species.[2,3] The Co 2p region (**Figure S14b**) for the CoS_x exhibits two main peaks at 782.4 and 798.2 eV that can be described to the +2 oxidation state of Co in CoS_x, which is consistent with previous XPS analysis.[1,4] **Figure S14c** show that XPS spectra of S 2p in CoS_x, the S 2p spectra were deconvoluted into two doublets under two constraints: the intensity ratio (1:2) and the binding energy difference (1.18 eV) between the $2p_{1/2}$ and $2p_{3/2}$ peaks, indicative of sulphur in S^{2-} and S_2^{2-} ions. Also, a peak observed at 169.2 eV corresponds to the binding energy of sulphur in sulphate (SO_4^{2-}) group.[4]

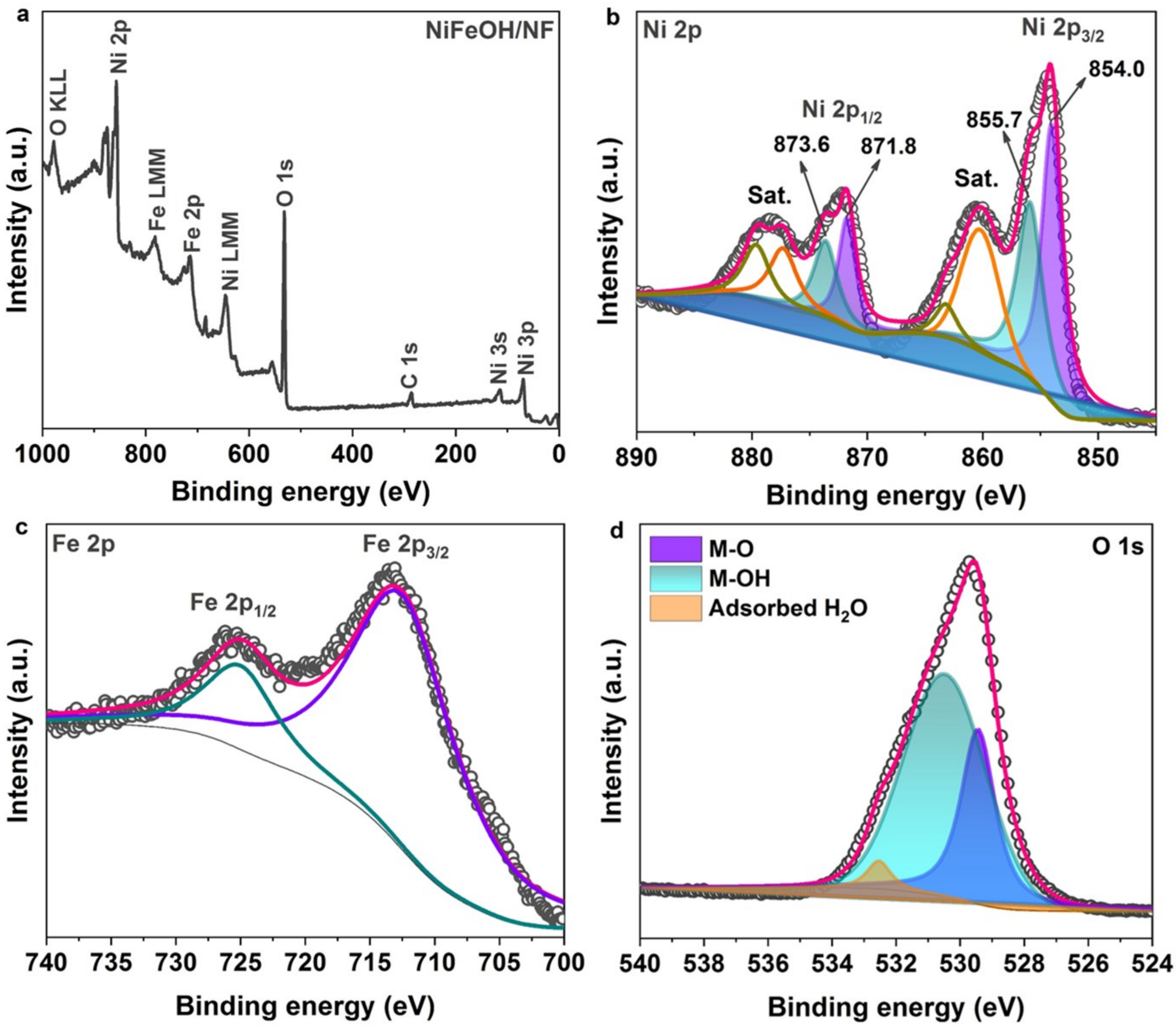

Figure S13. XPS spectra of NiFeOH/NF electrode. (a) Survey spectrum, (b) Ni 2p, (c) Fe 2p, (d) O 1s

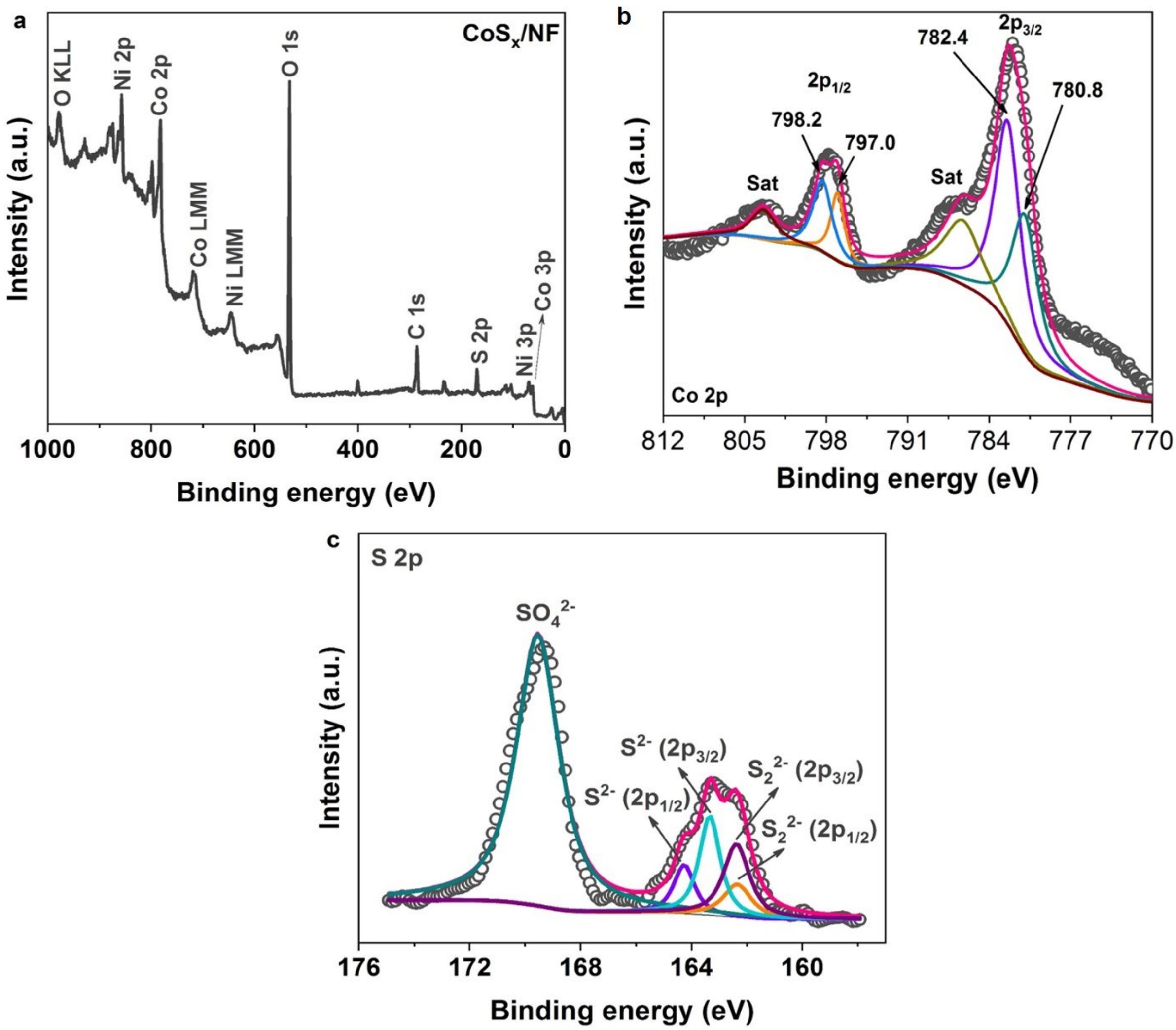

Figure S14. XPS spectra of CoS_x/NF electrode. (a) Survey spectrum, (b) Co 2p, (c) S 2p

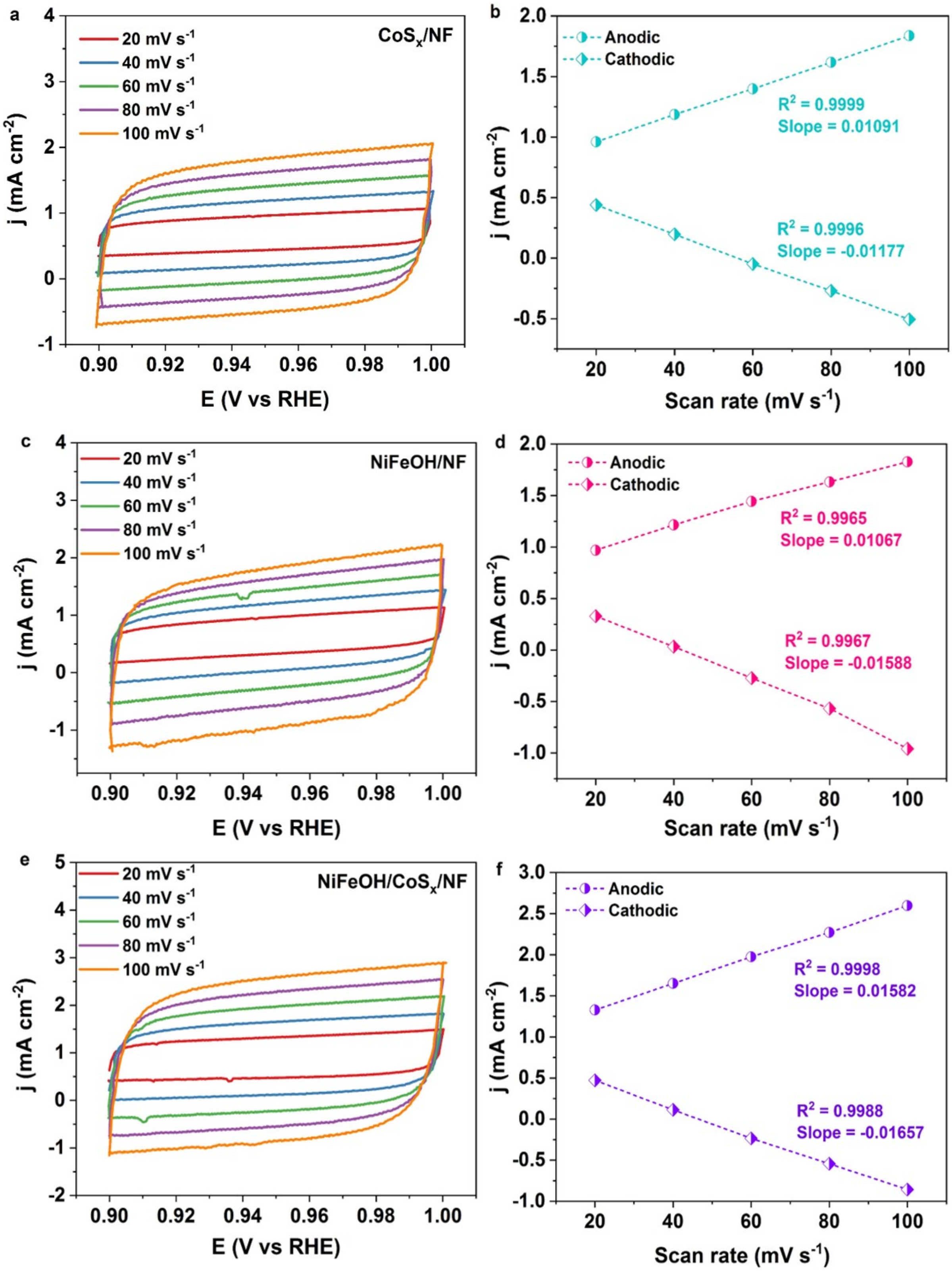

Figure S15. Double layer capacitance (C_{dl}) measurements for (a,b) CoS_x/NF, (c,d) NiFeOH/NF, (e,f) NiFeOH/CoS_x/NF electrode. CV scans measured at a potential range from 0.90 to 1.00 V vs RHE (no iR correction), where a capacitive current flows, with scan rates, respectively, 20, 40, 60, 80, and 100, mV s^{-1}.

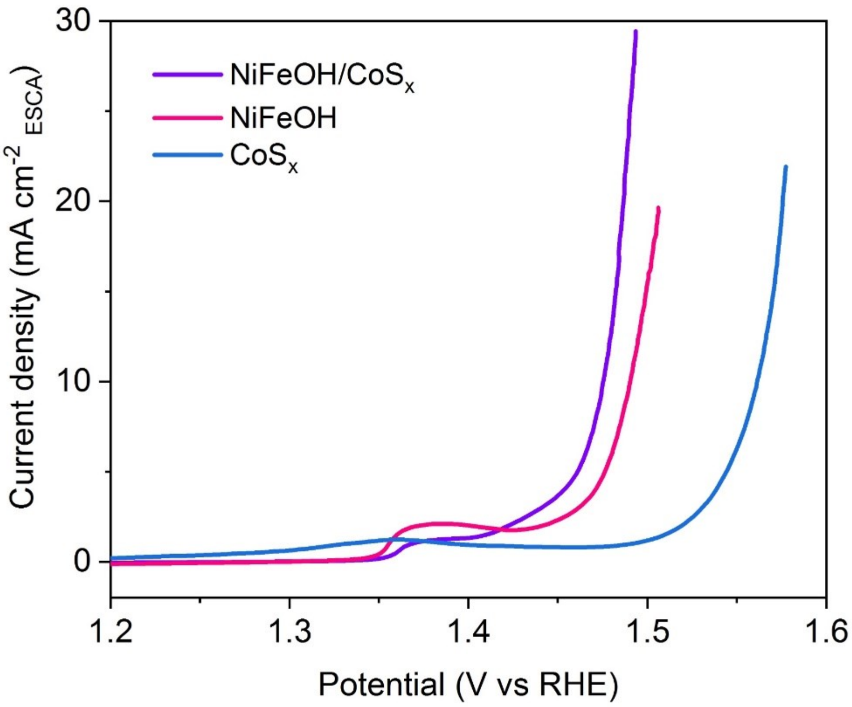

Figure S16. ECSA normalized polarization curves for as-prepared catalysts

Faradic efficiency calculation

The faradaic efficiency was calculated from the previous reported works:[3b]

Based on the amount of water displaced by the H_2/O_2 bubbles from the headspace of the inverted burette, the respective gas volumes are quantified. Ideal gas approximation was used at different time intervals to determine the moles of gas. From the total charge passed through the cell at various time intervals, the Faradic efficiency was calculated by the equation,

$$Faradaic\ efficiecny\ (FE) = \frac{n \times F \times m}{Q}$$

Where, n = number of electrons required for one molecule of H_2 or O_2, F = Faraday's constant, 96485 mol^{-1}, m = moles of gas evolved and Q is the total charge passed; Q = i.t.

$$FE\ \% = \frac{Experimental}{Theroretical} \times 100$$

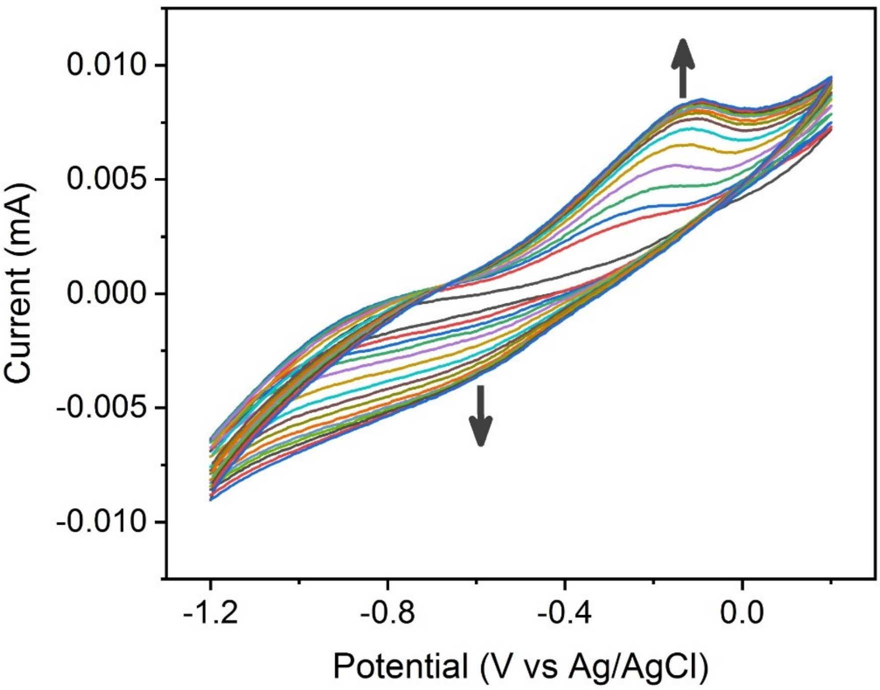

Figure S17. CV curves (15 cycles) during the electrodeposition of Co-S films on NF substrate at a scan rate of 5 mV s^{-1}.

Table S1. Comparison of the OER activity of NiFeOH/CoS_x/NF electrocatalysts in alkaline medium with some recently reported electrocatalysts

Catalyst	η_j (mV)	j (mA cm^{-2})	Tafel slope (mV/dec)	Reference
NiFeOH/CoS_x/NF	**209**	**50**	**39.1**	**This work**
	234	**100**		
FeCoNi-ATNs (H)/NF	225	10	40.2	Adv. Energy Mater. 2019, 9, 1901312
	340	50		
Ultrathin Ni-Fe LDHS	210	10	30	ACS Catal. 2019, 9, 6027.
Cr-doped FeNi–P/NCN	240	10	72.36	Adv. Mater. 2019, 31, 1900178
	290[a]	50		
$Fe_{0.5}Co_{0.5}P$	261	10	NA	ACS Catal. 2019, 9, 2956
	281[a]	50		
$NiCo_2S_4$/NF	243	10	54.9	Adv. Funct. Mater. 2019, 29, 1807031.
	320[a]	50		
Ni–Fe-LDH–MoS_2	250	10	45	ACS Energy Lett. 2018, 3, 952.
Ni–Al- LDH–MoS_2	310	10	56	
Ni_4Ce_1/CP	220	10	81.9	ACS Nano 2018, 12, 6245.
	278[a]	50		
$Mo_{51}Ni_{40}Fe_9$ nanobelts	257	10	51	ACS catal. 2019, 9, 1013.
Porous monolayer NiFe-LDH	230	10	47	Adv. Energy. Mater. 2019, 9, 1900881
	280[a]	50		
$Fe(PO_3)_2$-derived oxyhydroxide/NF	214[a]	50	51.9	Proc. Natl. Acad. Sci. USA. 2017. 114, 5607.
V-doped CoNiB/NF	370	100	NA	Adv. Energy Mater. 2019, 9, 1803799
Ni-Fe LDH/rGO	229[a]	50	39	Angew. Chem. Int. Ed. 2014, 53, 7584.
FeCoNi-ATNs/NF	295	10	52.7	Adv. Energy Mater. 2019, 9, 1901312
Gelled FeCoW	234[a]	50	37± 2	Science 2016, 352, 333.
Au@$CoFeO_x$/GC	328 ± 3	10	58	Nano Lett. 2017, 17, 6040
NiFe-DH/NF	323	10	77	ACS Energy Lett. 2017, 2, 1035.
NiFe LDH/Cu nanowire arrays	245[a]	50	27.8	Energy Environ. Sci. 2017, 10, 1820.
	281	100		
Fe-Doped β-$Ni(OH)_2$	219	10	53	ACS Energy Lett. 2019, 4, 622

	259[a]	50		
NiFe hydroxides/NF	215	10	28	Nat. Commun. 2015, 6, 6616.
	263[a]	50		
Ni_3FeN	280	10	46	Adv. Energy Mater. 2016, 6, 1502585
CeO_x/NiFe-OH/NF	249	20	43.2	ACS Sustainable Chem. Eng. 2019, 7, 16392.
	270[a]	50		
CeO_2/FeOOH	250	17.6	92.3	Adv. Mater. 2016, 28, 4698.
	279[a]	50		
CeO_2/Co_3O_4 interface nanotubes	265	10	68.1	ACS Catal. 2019, 9, 6484.
NiFe LDH/CNTs	247	10	31	J. Am. Chem. Soc. 2013, 135, 8452
	272[a]	50		
RuO_2/Ni	290	10	85	ACS Energy Lett. 2017, 2, 1035.
Fe_xN/graphene foam	238	10	44.5	ACS Catal. 2017, 7, 2052.
	278[a]	50		
Porous MoO_2/NF	280	20	NA	Adv. Mater. 2016, 28, 3785.
	297	50		
$NiCeO_x$–Au	271	10	NA	Nat. Energy 2016, 1, 16053
Co_4N nanowires/CC	308[a]	50	44	Angew. Chem. Int. Ed. 2015, 54, 14710.
$CoNi(OH)_x$/Cu foil	313[a]	50	77	Adv. Energy Mater. 2016, 6, 1501661.
Ni_2P nanoparticle/GC	320[a]	50	NA	Energy Environ. Sci. 2015, 8, 2347.
NiFe LDH/MW-graphene	335[a]	50	38	Science 2016, 353, 1413.
Porous Ni-P nanoplates/GC	300	10	64	Energy Environ. Sci. 2016, 9, 1246.
	350[a]	50		
NiFeP/Ni	270	10	59	ACS Energy Lett. 2017, 2, 1035.
CoFePO/Ni	274	10	51.7	ACS Nano. 2016, 10, 8738.
$Ni_xFe_{3-x}O_4$/Ni	225	10	44	ACS Energy Lett. 2018, 3, 1698.
CoNi(20:1)-P/GC	273	10	45	Energy Environ. Sci. 2017, 10, 893
$Co_{0.85}Se$|CoP/CFP	240	10	46	Part. Part. Syst. Charact. 2018, 1800135

a: The value is estimated from the polarization curves shown in the literatures

Table S2. Comparison of the HER activity of NiFeOH/CoS_x/NF electrocatalysts in alkaline medium with some recently reported electrocatalysts

*Electrolyte: 1 M NaOH

Catalyst	η_j (mV)	j (mA cm^{-2})	Tafel slope (mV/dec)	Reference
NiFeOH/CoS$_x$/NF	**146**	**10**	**121.3**	**This work**
Ni−Fe-LDH−MoS$_2$	180	10	82	ACS Energy Lett. 2018, 3, 952.
FeCo/CP	149	10	77	ACS Catal. 2017, 7, 469
FeCoNi-ATNs/NF	150	10	107	Adv. Energy Mater. 2019, 9, 1901312
Ni$_5$P$_4$ /Nickel foil	150	10	53	Angew. Chem. Int. Ed. 2015, 127, 12538
Cr-doped FeNi–P/NCN	190	10	68.51	Adv. Mater. 2019, 31, 1900178
MoC$_x$	151	10	59	Nat Commun 2015, 6, 6512.
Co@N-CS/N-HCP@CC (A-S-720)	154	10	81	Adv. Energy Mater. 2019, 9, 1803918
NiCo$_2$O$_4$/NF	164	10	107	Adv. Funct. Mater. 2016, 26, 3515.
Co$_1$Mn$_1$CH/NF	180	10	NA	J. Am. Chem. Soc. 2017, 139, 8320
Porous NiSe$_2$ nanosheets/CP	184	10	77	Chem. Mater. 2015, 27, 5702-5711.
Co$_9$S$_8$@MoS$_2$/CNFs	190	10	110	Adv. Mater. 2015, 27,4752
CoSe$_2$/carbon cloth	190	10	85	Adv. Mater. 2016, 28, 7527
FeNi@NC/CNT	202	10	113.7	Angew. Chem. Int. Ed. 2018, 57, 8921
Co$_{0.75}$Fe$_{0.25}$@NC	202	10	68	J. Power Sources 2018, 389, 249
Co-MoS$_2$/CC	203	10	158	Energy. Environ. Sci. 2016, 9, 2789
CoP/CC	209	10	129	J. Am. Chem. Soc. 2014, 136, 7587.
NiFe LDHs/NF	210*	10	NA	Science 2014, 345, 1593-1596.
Ni$_2$P	220	10	NA	Energy Environ. Sci. 2015, 8, 2347.
Cu$_{0.3}$Co$_{2.7}$P/NC	220	10	122	Adv. Energy. Mater. 2017, 7, 1601555
Ni$_3$S$_2$/NF	223	10	NA	J.Am.Chem.Soc.2015,137,14023

Table S3: Chemical states and peak position of NiFeOH/CoS$_x$ catalyst

Sample	Elements	Chemical state	Binding energy (eV)
$NiFeOH/CoS_x$ (as-prepared catalyst)	Co	Co^{3+} $2p_{3/2}$	779.2
		Co^{2+} $2p_{3/2}$	780.7
		Co^{3+} $2p_{1/2}$	794.8
		Co^{2+} $2p_{1/2}$	796.2
	Ni	Ni^{2+} $2p_{3/2}$	855.8
		Ni^{2+} $2p_{1/2}$	873.4
	Fe	Fe^{3+} $2p_{3/2}$	713.4
		Fe^{3+} $2p_{1/2}$	726.3
	O	O^{I}	529.9
		O^{II}	531.3
		O^{III}	532.6
		O^{IV}	533.4
	S	S $2p_{3/2}$	162.0
		S $2p_{1/2}$	163.2
		S^{6+} $2p_{3/2}$	168.1
		S^{6+} $2p_{1/2}$	170.3

Table S4. Comparison of TOFs of $NiFeOH/CoS_x/NF$ electrocatalysts in alkaline medium with other reported works.

Electrocatalysts	**TOF**	**Reference**
$NiFeOH/CoS_x$	**$0.52\ s^{-1}$ at $\eta = 200$ mV**	**This work**
$NiCeO_x$–Au	$0.0795\ s^{-1}$ at $\eta = 280$ mV	Nat. Energy 2016, 1, 16053
V-CoNiB	$0.09\ s^{-1}$ at $\eta = 400$ mV	Adv. Energy Mater. 2019, 9, 1803799
$Fe(PO_3)_2/Ni_2P$	$0.12\ s^{-1}$ at $\eta = 300$ mV	Proc. Natl. Acad. Sci. USA. 2017. 114, 5607.
Pt/C	$0.0053\ s^{-1}$ at $\eta = 350$ mV	J. Am. Chem. Soc. 2014, 136, 7077
Ni, Fe (OOH)	$0.073\ s^{-1}$ at $\eta = 300$ mV	Energy Environ Sci. 2018, 11, 2858
Ru^0/CeO_2	$0.004\ s^{-1}$ at $\eta = 350$ mV	J. Colloid Interface Sci. 2019, 534, 704
CeO_2/ Co_3O_4	$0.029\ s^{-1}$ at $\eta = 340$ mV	ACS Catal. 2019, 9, 6484−6490
CeO_x/NiFeOH	$0.0684\ s^{-1}$ at $\eta = 280$ mV	ACS Sustainable Chem. Eng. 2019, 7, 16392
$NiCeO_x$–GC	$0.0052\ s^{-1}$ at $\eta = 280$ mV	Nat. Energy 2016, 1, 16053
RuO_2	$0.0104\ s^{-1}$ at $\eta = 350$ mV	J. Am. Chem. Soc. 2014, 136, 7077
γ-CoOOH	$0.09\ s^{-1}$ at $\eta = 300$ mV	J. Am. Chem. Soc. 2013, 135, 8452
Fe–Co_3O_4@Fe–Co–Bi/CC	$0.14\ s^{-1}$ at $\eta = 400$ mV	J. Mater. Chem. A 2017, 5, 6388

Table S5. Comparison of overall water splitting performance of NiFeOH/CoS_x/NF electrode with other reported bifunctional electrodes tested under similar conditions.

Electrocatalysts	**Substrate**	**$\eta_{10,\ overall}$ (V)**	**Electrolyte**	**Reference**
NiFeOH/CoS_x/NF	**Nickel foam**	**1.563**	**1.0 M KOH**	**This work**
PO-Ni/Ni-NCNFs	Carbon nanofibers	1.69	1.0 M KOH	Nano Energy, 2018, 51, 286.
NiFe LDH/NF	Nickel foam	1.70	1.0 M KOH	Science 2014, 345, 1593.
NiMo/NiMoO@NC	Nickel foam	1.57	1.0 M KOH	Small 2017, 13, 1702018
CoS_x/Ni_3S_2@NF	Nickel foam	1.572	1.0 M KOH	ACS Appl. Mater. Interfaces 2018, 10, 27712.
NiFe@NC@NF	Nickel foam	1.58	1.0 M KOH	ACS Catal. 2016, 6, 580
FeNi(BDC)(DMF,F)/NF	Nickel foam	1.58	1.0 M KOH	Applied Catalysis B: Environmental, 2019, 258, 118023
NiCoP/SCW	Scrapped Copper wire	1.59	1.0 M KOH	Adv. Energy Mater. 2018, 8, 1802615.
FeCoP UNSAs/NF	Nickel foam	1.60	1.0 M KOH	Nano energy 2017, 41, 583.
$NiCo_2S_4$NW/NF	Nickel foam	1.63	1.0 M KOH	Adv. Funct. Mater. 2016, 26, 4661.
CoFeO@N/S-rGO	Carbon paper	1.63	1.0 M KOH	J. Mater. Chem. A 2018, 6, 15728.
CoP/NCNHP	Carbon paper	1.64	1.0 M KOH	J. Am. Chem. Soc., 2018, 140, 7.
Fe-Ni@NCCNTs	Nickel foam	1.64	1.0 M KOH	Angew. Chem., 2018, 57, 8921.
NiFe/$NiCo_2O_4$/ Ni	Nickel foam	1.67	1.0 M KOH	Adv. Funct. Mater. 2016, 26, 3515
FeCoNi@NCP	Carbon paper	1.687	1.0 M KOH	ACS Catal. 2017, 7, 469
Co_1Mn_1CH/NF	Nickel foam	1.68	1.0 M KOH	J. Am. Chem. Soc., 2017, 139, 8320-8328.
$Co(OH)_2$@NCNTs@NF	Nickel foam	1.72	1.0 M KOH	Nano Energy, 2018, 47, 96-104

Reference

[1] a) Y. Sun, C. Liu, D. C. Grauer, J. Yano, J. R. Long, P. Yang, C. J. Chang, *J. Am. Chem. Soc.* 2013, **135**, 17699; b) N. Kornienko, J. Resasco, N. Becknell, C.-M. Jiang, Y.-S. Liu, K. Nie, X. Sun, J. Guo, S. R. Leone, P. Yang, *J. Am. Chem. Soc.* 2015, **137**, 7448.

[2] a) H. Liang, A. N. Gandi, C. Xia, M. N. Hedhili, D. H. Anjum, U. Schwingenschlögl, H. N. Alshareef, *ACS Energy Lett.* 2017, **2**, 1035; b) H. Zhou, F. Yu, J. Sun, R. He, S. Chen, C.-W. Chu, Z. Ren, *Proc. Natl. Acad. Sci. U. S. A.* 2017, **114**, 5607; c) Q. Zhang, N. M. Bedford, J. Pan, X. Lu, R. Amal, *Adv. Energy Mater.* 2019, **9**, 1901312; d) Z. Qiu, C.-W. Tai, G. A. Niklasson, T. Edvinsson, *Energy Environ. Sci.* 2019, **12**, 572.

[3] a) R. Bose, V. R. Jothi, D. B. Velusamy, P. Arunkumar, S. C. Yi, *Part. Part. Syst. Charact.* 2018, **35**, 1800135; b) V. R. Jothi, R. Bose, H. Rajan, C. Jung, S. C. Yi, *Adv. Energy Mater.* 2018, **8**, 1802615; c) R. Bose, K. Karuppasamy, H. Rajan, D. B. Velusamy, H.-S. Kim, A. Alfantazi, *ACS Sustainable Chem. Eng.* 2019, **7**, 16392.

[4] a) R. Bose, Z. Jin, S. Shin, S. Kim, S. Lee, Y.-S. Min, *Langmuir* 2017, **33**, 5628; b) R. Bose, M. Seo, C.-Y. Jung, S. C. Yi, *Electrochim. Acta* 2018, **271**, 211.